Celal Bayar University Journal of Science
Volume 13, Issue 4, p 851-861

Structure, Spectroscopic and Quantum Chemical Investigations of 4-Amino-2-Methyl-8-(Trifluoromethyl)Quinoline

*T. Raci Sertbakan

Department of Physics, Faculty of Art and Science, Ahi Evran University, 40100, Kırsehir, Turkey,
trsertbakan@ahievran.edu.tr
*Corresponding Author

Received: 18 June 2017
Accepted: 31 October 2017
DOI: 10.18466/cbayarfbe.339858

Abstract

This work deals with the spectroscopic properties (FT-IR, FT-Raman and NMR), structural and some electronic properties as well as theoretical calculations of 4-amino-2-methyl-8-(trifluoromethyl) quinoline (AMTQ) molecule. The vibrational, structural and some electronic properties observations of the AMTQ were reported, which is investigated using some spectral methods and DFT calculations. FT-IR and FT-Raman spectra were obtained for AMTQ at room temperature in the region 4000 cm^{-1}- 400 cm^{-1} and 3500-50 cm^{-1}, respectively. In the DFT calculations, the B3LYP functional with cc-pVDZ, cc-pVTZ and cc-pVQZ basis sets was applied to carry out the quantum mechanical calculations of the spectroscopic, structural and some electronic properties of AMTQ. FT-IR and FT-Raman spectra were interpreted with the by using of normal coordinate analysis based on scaled quantum mechanical force field. The present work expands our understanding of the both the vibrational and structural properties as well as some electronic properties of the AMTQ by means of the theoretical and experimental methods.

Keywords: 4-amino-2-methyl-8-(trifluoromethyl)quinoline, FT-IR and FT-Raman spectra, NMR spectra, DFT, Electronic properties

1. Introduction

Quinoline and its derivatives possess an aromatic heterocyclic unit of benzene connected to a pyridine ring. It is a heterocyclic aromatic organic compound with the chemical formula C_9H_7N. It is a colorless hygroscopic liquid with a strong odor. Aged samples, especially if exposed to light, become yellow and later brown. Quinoline is only slightly soluble in cold water but dissolves readily in hot water and most organic solvents. Quinoline itself has few applications, but many of its derivatives are useful in diverse applications [1].

In addition to the medicinal and therapeutic applications of quinoline derivatives, these compounds have also shown technological properties. Because, it has the unique structural and electronic properties. Quinoline and its derivatives presents the electronic delocalization and material nonlinear optical properties in the manifestation of fluorescence effects [2]. They were given the important developments in the field of organic light emitting diodes [3–5].

Vibrational spectroscopy in combination with computational chemistry has been used systematically over the past decade to elucidate the spectroscopic, structures and some electronic properties of molecule. Various researchers [6-11] used simulation methods such as DFT, HF simulations to explained molecular structure and vibrational spectra. Such study supports the experimental data in interpreting the calculations results of the structural and spectroscopic properties of the isolated molecule. Erdogdu et al. [12-15] studied vibrational properties of the several molecules. Experimental results were favorable agreed with the results obtained by simulations.

Quinoline derivatives has been applied the characterize by Raman spectroscopy [16,17,20–22]. Especially, aminoquinolines have chromophoric groups and highly symmetric molecular structures. Therefore, they give rise to intense Raman signals [16,18,19,23,24]. The vibrational spectra of the some substituted quinolones have been experimentally recorded and theoretically analyzed [21,25–27]. It is reported that the solid state structure for 4,7- dichloroquinoline has been described [28]. In that work, Authors showed the two molecules with the quinolone asymmetric unit. That compounds have the crystallizes in a monoclinic system with $P_{21/n}$ space group. Some quinolone derivative such as 4,7-dichloroquinoline and quinolin-8-ol, and 4-azido-7-

chloroquinoline molecules have been characterized by the Raman and infrared spectra. In that work, the 4-azido-7-chloroquinoline compound was synthesized from 4,7-dichloroquinoline according to the method described by Pereira et al. [29]. The molecular structure and vibrational spectra of these molecules have been calculated by DFT (B3LYP with 6-311++G(d,p)).

2. Theoretical and Experimental Details

Density functional theory (DFT) computations for the geometric optimization and frequency calculation were performed using Gaussian 09 program [30]. The calculations employed the B3LYP exchange-correlation functional, which combines the hybrid exchange functional of Becke with the gradient-correlation functional of Lee et al. and the cc-pVDZ, cc-pVTZ and cc-pVQZ basis set. Calculations were based on the isolated molecule model, so the environmental effects were not considered. The optimal geometry was determined by minimizing the energy with respect to all geometrical parameters without imposing molecular symmetry constraints. In the optimized structure, imaginary frequency modes were absent which provided a true minimum picture of the potential energy surface.

Following the geometry optimizations with B3LYP method, the optimized structural parameters used in the vibrational wavenumber calculation at DFT level to characterize all stationary points while minima. The potential energy distribution (PED) was calculated by using the scaled quantum mechanics (SQM) program [31] and the fundamental vibrational modes were characterized by their PED values. In addition, the frontier molecular orbital analysis and Molecular electrostatic potential (MEP) were performed.

AMTQ was purchased from Aldrich and used without further purification. Infrared spectra of the samples were recorded between for the 400-4000 cm^{-1} on a Mattson 1000 FTIR spectrometer which was calibrated using polystyrene bands. The samples were prepared as a KBr disc. FT-Raman spectrum of AMTQ has been recorded in the frequency region 50–3500 cm^{-1} on a Thermo Scientific DXR Raman Microscope with Nd: YVO_4 DPSS laser operating with 532 nm excitation. The sample was prepared as a KBr disc. The ^{13}C NMR spectra were recorded in chloroform solutions and all signals are referenced to TMS on a Bruker Ultrashield FT-NMR Spectrometer. All NMR spectra were measured at room temperature.

3. Molecular structure

The optimized structure of conformer of AMTQ was shown in Figure 1 which has the atom numbering scheme adopted in this study. The optimized structural parameters such as dihedral angles, bond angles and bond lengths of the AMTQ were given in Table 1.

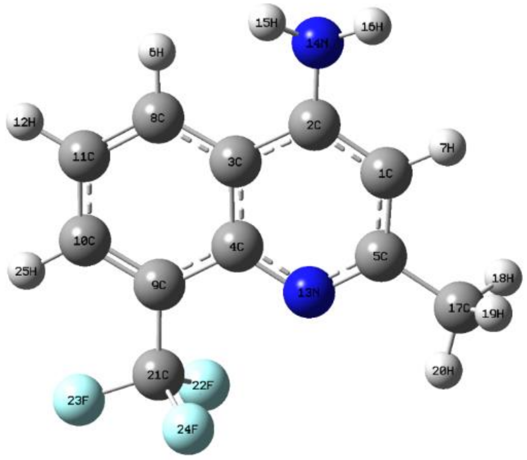

Figure 1. Molecular structure and atomic numbering of the 4-amino-2-methyl-8-(trifluoromethyl)quinoline molecule.

4. Assignment of Vibrational Spectra

In order to assist in the assignment of the vibrational bands, predicted infrared and Raman spectra obtained by using DFT approximation. The AMTQ molecule consists of 25 atoms. So, it has 69 normal vibrational modes. Since it belongs to the Cs point group, these normal modes are distributed with 45 in-plane and 24 out-of-plane vibrations. The experimental and calculated infrared and Raman spectra for AMTQ are given in Figures 2 and 3. The corresponding data are gathered in Table 2.

The NH stretching vibrations give rise to bands at 3500-3300 cm^{-1} [32]. According to Roeges, the N–H stretching vibration appears strongly and broadly in the region 3390 ± 60 cm^{-1} [33]. For the title compound N-H stretching modes are assigned at 3383 and 3494 cm^{-1} theoretically (cc-pVQZ) and a strong band is observed in the IR spectrum at 3383 cm^{-1} (FT-IR) 3388 cm^{-1} (FT-Raman). It is well-known that the amino group presents a characteristic band in the 1500-1600 cm^{-1} range of the IR spectrum, originated by the NH_2 deformation mode (δ_{NH2}). The NH_2 deformation band of the title compound detected at 1592 cm^{-1} (FT-IR) and 1594 cm^{-1} (FT-Raman). 1585 cm^{-1} peak predicted as the NH_2 deformation band by means of B3LYP/cc-pVQZ level of theory.

The C-H stretching vibrations of the aromatic structure appear in the region 3200-3000 cm^{-1}. It's characteristic region for the identification of the C-H stretching vibrations [6-11]. The ring, which is coordinated trifluoromethyl group, has the three CH stretching vibrations. 3072 cm^{-1}, 3091 cm^{-1} and 3114 cm^{-1} peaks were predicted the CH stretching vibrations by the B3LYP/cc-pVQZ calculation. According to the PED results, PED contributions were almost calculated as pure modes. In the FT-Raman spectra, CH stretching

Celal Bayar University Journal of Science
Volume 13, Issue 4, p 851-861

vibrations of this ring were observed at 3072 cm^{-1} and 3099 cm^{-1}.

Experimentally, the in-plane CH bending modes were measured at 1517/1525 cm^{-1} (IR/Raman), 1442/1441cm^{-1} (IR/Raman) and -/1309 (-/Raman) cm^{-1}, -/1259 cm^{-1} (-/Raman) 1228/1228 cm^{-1} (IR/Raman), 1189/1182 cm^{-1} (IR/Raman) and 1143/1144 cm^{-1} (IR/Raman), whereas computed in-plane CH bending modes were found at 1501 cm^{-1}, 1441 cm^{-1}, 1320 cm^{-1}, 1252 cm^{-1}, 1209 cm^{-1}, 1170 cm^{-1} and 1161 cm^{-1} by DFT (B3LYP/cc-pVQZ) calculation. Additionally, the out of plane bending CH modes were observed at 842 (836) cm^{-1}, 825 cm^{-1} and 771 (762) cm^{-1} in the FT-IR (FT-Raman) spectra.

The identification of C-N vibration is a very difficult task, since the mixing of several bands is possible in this region. However, with the help of theoretical calculation (DFT), the C-N stretching vibrations are calculated. Several bands observed at 1375 1077 cm^{-1} in the FT-Raman spectrum of the studied compound, with counterpart at 1076 cm^{-1} in the infrared spectrum are assigned to the C-N stretching vibrations. The IR band observed at 1569 cm^{-1}, 1619 cm^{-1} and 1638 cm^{-1} assigned to the CC stretching vibrations. Their corresponding counterpart detected at 1572 cm^{-1}, 1621 cm^{-1} and 1637cm^{-1} in the FT-Raman spectra. These vibrations calculated at 1557 cm^{-1}, 1615 cm^{-1} and 1603 cm^{-1} by means of B3LYP/cc-pVQZ level of theory. PED contribution of these vibrations predicted as mixed with CCC, CCH bending vibrations.

The C-H stretching frequencies of methyl group appear just below 3000 cm^{-1} [34,35]. The title molecule possesses methyl (-CH_3) group. The strong and distinct C-H stretching band at 2924/2925 cm^{-1} (FT-IR / FT-Raman) and 2956/2964 cm^{-1} (FT-IR / FT-Raman) are in agreement with the theoretical values of 2933 cm^{-1} (mode no: 61) and 2979 cm^{-1} (mode no:62) by B3LYP/cc-pVQZ method and are well supported by the PED values. The asymmetric and symmetric bending vibrations of methyl groups normally appear in the around 1450 cm^{-1} and around 1350 cm^{-1} region, respectively [34,35]. In the present study, asymmetric CH_3 bending vibration (mode no 27) was observed at 1434 cm^{-1} in the FT-Raman spectrum as very week band and its corresponding counterpart couldn't be detected in the FT-IR spectrum. Asymmetric CH_3 bending mode of the methyl group was also predicted at 1423 cm^{-1} at the B3LYP with cc-pVQZ level of theory. 1421 cm^{-1} (FT-IR and FT-Raman) peak was assigned to the asymmetric bending vibration of the CH_3 group. Symmetric CH3 peak was calculated at 1333 cm^{-1} at the B3LYP/cc-pVQZ level of theory. This vibration was measured at 1332 cm^{-1} in the FT-IR spectra.

The band at 1117 cm^{-1} in the FT-IR spectrum was appointed as C-F stretching vibration. This mode was predicted 1112 cm^{-1}. According to the calculations 1140 cm^{-1} and 717 cm^{-1} are assigned to the symmetric C-F_3 stretching modes, while the 1132 cm^{-1}vibration is the asymmetric C-F_3 stretching mode. In the predicted spectra, out-of plane F-C-F bending vibration is appointed at 656 cm^{-1} with 31% contributions of PED.

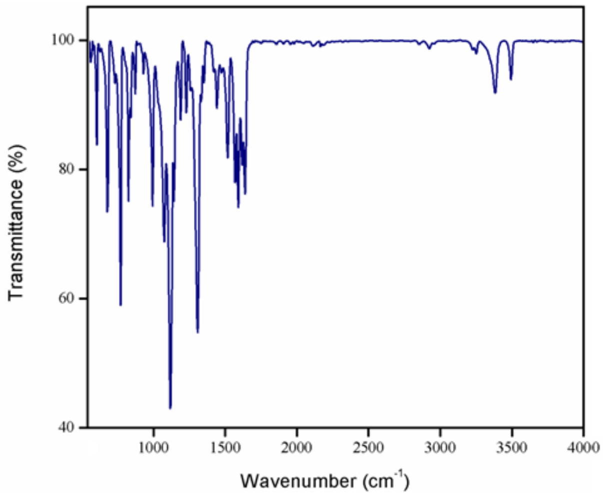

Figure 2. Experimental Infrared spectra of 4-amino-2-methyl-8-(trifluoromethyl)quinoline molecule

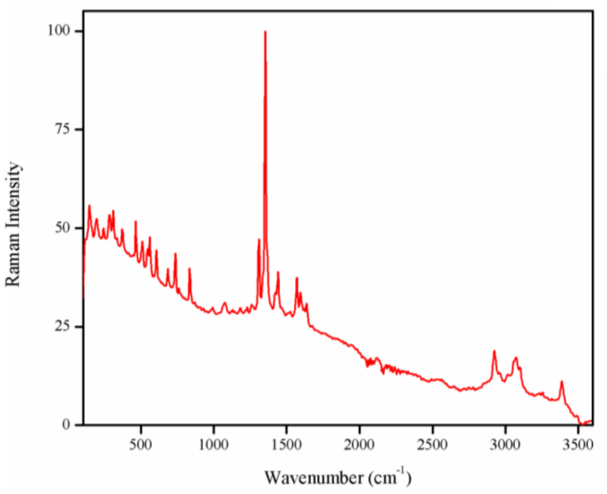

Figure 3. Experimental Raman spectra of 4-amino-2-methyl-8-(trifluoromethyl)quinoline molecule

Table 1. Optimized geometric parameters of 4-amino-2-methyl-8-(trifluoromethyl)quinoline

Bond Lengths (Å)	cc-pVDZ	cc-pVTZ	cc-pVQZ	Bond Angles (º)	cc-pVDZ	cc-pVTZ	cc-pVQZ	Dihedral Angels (º)	cc-pVDZ	cc-pVTZ	cc-pVQZ
C_1-C_2	1.387	1.387	1.378	$C_2-C_1-C_5$	120.3	120.3	120.4	$C_5-C_1-C_2-C_3$	-0.999	1.013	0.674
C_1-C_5	1.417	1.417	1.409	$C_2-C_1-H_7$	119.9	119.9	120.0	$C_5-C_1-C_2-N_{14}$	-178.2	178.3	178.2
C_1-H_7	1.093	1.093	1.082	$C_5-C_1-H_7$	119.6	119.6	119.5	$H_7-C_1-C_2-C_3$	179.8	-179.8	-179.8
C_2-C_3	1.440	1.440	1.432	$C_1-C_2-C_3$	117.7	117.7	117.8	$H_7-C_1-C_2-N_{14}$	2.531	-2.525	-2.262
C_2-N_{14}	1.384	1.384	1.377	$C_1-C_2-N_{14}$	121.7	121.8	121.3	$C_2-C_1-C_5-N_{13}$	-0.727	0.736	0.611
C_3-C_4	1.432	1.432	1.423	$C_3-C_2-N_{14}$	120.4	120.4	120.7	$C_2-C_1-C_5-C_{17}$	179.9	-179.9	-179.5
C_3-C_8	1.418	1.418	1.411	$C_2-C_3-C_4$	117.1	117.1	117.1	$H_7-C_1-C_5-N_{13}$	178.4	-178.4	-178.8
C_4-C_9	1.432	1.432	1.426	$C_2-C_3-C_8$	123.1	123.1	123.2	$H_7-C_1-C_5-C_{17}$	-0.887	0.897	0.957
C_4-N_{13}	1.362	1.362	1.355	$C_4-C_3-C_8$	119.6	119.6	119.6	$C_1-C_2-C_3-C_4$	2.055	-2.081	-1.530
C_5-N_{13}	1.324	1.324	1.316	$C_3-C_4-C_9$	118.0	118.0	118.0	$C_1-C_2-C_3-C_8$	-177.2	177.2	178.1
C_5-C_{17}	1.508	1.508	1.504	$C_3-C_4-N_{13}$	123.5	123.5	123.1	$N_{14}-C_2-C_3-C_4$	179.3	-179.4	-179.1
H_6-C_8	1.092	1.092	1.081	$C_9-C_4-N_{13}$	118.3	118.3	118.7	$N_{14}-C_2-C_3-C_8$	0.093	-0.121	0.600
C_8-C_{11}	1.380	1.380	1.371	$C_1-C_5-N_{13}$	123.2	123.2	122.9	$C_1-C_2-N_{14}-H_{15}$	-149.4	149.4	155.1
C_9-C_{10}	1.382	1.382	1.373	$C_1-C_5-C_{17}$	119.6	119.6	119.6	$C_1-C_2-N_{14}-H_{16}$	-15.91	15.89	15.32
C_9-C_{21}	1.512	1.512	1.512	$N_{13}-C_5-C_{17}$	117.0	117.0	117.3	$C_3-C_2-N_{14}-H_{15}$	33.31	-33.28	-27.30
$C_{10}-C_{11}$	1.412	1.412	1.404	$C_3-C_8-H_6$	119.9	119.9	120.2	$C_3-C_2-N_{14}-H_{16}$	166.8	-166.8	-167.1
$C_{10}-H_{25}$	1.089	1.090	1.079	$C_3-C_8-C_{11}$	121.7	120.7	120.8	$C_2-C_3-C_4-C_9$	178.7	-178.6	-178.9
$C_{11}-H_{12}$	1.091	1.091	1.080	$H_6-C_8-C_{11}$	119.1	119.1	118.8	$C_2-C_3-C_4-N_{13}$	-1.629	1.647	1.283
$N_{14}-H_{15}$	1.014	1.014	1.004	$C_4-C_9-C_{10}$	120.	120.6	120.6	$C_8-C_3-C_4-C_9$	-1.982	1.995	1.333
$N_{14}-H_{16}$	1.015	1.015	1.005	$C_4-C_9-C_{21}$	119.7	119.7	119.8	$C_8-C_3-C_4-N_{13}$	177.6	-177.6	-178.4
$C_{17}-H_{18}$	1.103	1.103	1.091	$C_{10}-C_9-C_{21}$	119.5	119.5	119.0	$C_2-C_3-C_8-H_6$	2.444	-2.459	-2.132
$C_{17}-H_{19}$	1.103	1.103	1.092	$C_9-C_{10}-C_{11}$	120.7	120.7	120.8	$C_2-C_3-C_8-C_{11}$	-179.0	179.0	179.2
$C_{17}-H_{20}$	1.097	1.097	1.086	$C_9-C_{10}-H_{25}$	119.3	119.3	119.6	$C_4-C_3-C_8-H_6$	-176.8	176.8	177.5
$C_{21}-F_{22}$	1.348	1.349	1.345	$C_{11}-C_{10}-H_{25}$	119.8	119.8	119.5	$C_4-C_3-C_8-C_{11}$	1.647	-1.656	-1.078
$C_{21}-F_{23}$	1.361	1.361	1.356	$C_8-C_{11}-C_{10}$	120.0	120.0	120.0	$C_3-C_4-C_9-C_{10}$	0.987	-0.994	-0.675
$C_{21}-F_{24}$	1.349	1.348	1.345	$C_8-C_{11}-H_{12}$	120.3	120.3	120.3	$C_3-C_4-C_9-C_{21}$	-179.2	179.2	179.5
				$C_{10}-C_{11}-H_{12}$	119.6	119.6	119.6	$N_{13}-C_4-C_9-C_{10}$	-178.6	178.6	179.1
				$C_4-N_{13}-C_5$	117.8	117.8	118.4	$N_{13}-C_4-C_9-C_{21}$	1.015	-1.031	-0.678
				$C_2-N_{14}-H_{15}$	116.2	116.2	117.9	$C_3-C_4-N_{13}-C_5$	-0.026	0.029	-0.054
				$C_2-N_{14}-H_{16}$	115.0	115.0	116.3	$C_9-C_4-N_{13}-C_5$	179.6	-179.6	-179.8
				$H_{15}-N_{14}-H_{16}$	111.8	111.8	113.4	$C_1-C_5-N_{13}-C_4$	1.244	-1.261	-0.924
				$C_5-C_{17}-H_{18}$	110,8	111.0	111.1	$C_{17}-C_5-N_{13}-C_4$	-179.3	179.3	179.2
				$C_5-C_{17}-H_{19}$	111.0	110.8	110.6	$C_1-C_5-C_{17}-H_{18}$	-61.64	-57.35	-52.99

				C_5-C_{17}-H_{20}	109.6	109.6	109.8	C_1-C_5-C_{17}-H_{19}	57.27	61.57	66.02
				H_{18}-C_{17}-H_{19}	107.0	107.0	107.2	C_1-C_5-C_{17}-H_{20}	177.9	-178.0	-173.9
				H_{18}-C_{17}-H_{20}	108.9	109.1	109.2	N_{13}-C_5-C_{17}-H_{18}	118.9	122.0	126.8
				H_{19}-C_{17}-H_{20}	109.1	108.9	108.7	N_{13}-C_5-C_{17}-H_{19}	-122.1	-119.0	-114.1
				C_9-C_{21}-F_{22}	112.5	112.5	112.5	N_{13}-C_5-C_{17}-H_{20}	-1.427	1.347	5.899
				C_9-C_{21}-F_{23}	111.0	111.0	111.1	C_3-C_8-C_{11}-C_{10}	-0.255	0.252	0.122
				C_9-C_{21}-F_{24}	112.5	112.6	112.6	C_3-C_8-C_{11}-H_{12}	-179.7	179.7	179.7
				F_{22}-C_{21}-F_{23}	106.3	106.3	106.1	H_6-C_8-C_{11}-C_{10}	178.2	-178.2	-178.5
				F_{22}-C_{21}-F_{24}	107.5	107.5	107.6	H_6-C_8-C_{11}-H_{12}	-1.267	1.271	1.066
				F_{23}-C_{21}-F_{24}	106.3	106.3	106.2	C_4-C_9-C_{10}-C_{11}	0.388	-0.392	-0.270
								C_4-C_9-C_{10}-H_{25}	179.8	-179.8	-179.8
								C_{21}-C_9-C_{10}-C_{11}	-179.3	179.3	179.5
								C_{21}-C_9-C_{10}-H_{25}	0.125	-0.122	-0.073
								C_4-C_9-C_{21}-F_{22}	-61.38	-60.41	-60.58
								C_4-C_9-C_{21}-F_{23}	179.4	-179.4	-179.5
								C_4-C_9-C_{21}-F_{24}	60.38	61.35	61.37
								C_{10}-C_9-C_{21}-F_{22}	118.3	119.8	119.6
								C_{10}-C_9-C_{21}-F_{23}	-0.814	0.784	0.625
								C_{10}-C_9-C_{21}-F_{24}	-119.8	-118.3	-118.4
								C_9-C_{10}-C_{11}-C_8	-0.777	0.786	0.563
								C_9-C_{10}-C_{11}-H_{12}	178.7	-178.7	-179.0
								H_{25}-C_{10}-C_{11}-C_8	179.7	-179.7	-179.8
								H_{25}-C_{10}-C_{11}-H_{12}	-0.721	0.728	0.534

Table 2. Vibrational assignment of 4-amino-2-methyl-8-(trifluoromethyl)quinoline by normal mode analysis based on SQM force field calculations.

Theoretical (B3LYP)							Experimental		PED(%)[c]
		cc-pVDZ			cc-pVTZ	cc-pVQZ			
Normal Modes		Freq.[a]	I_{IR}[b]	I_{Raman}[b]	Freq.[a]	Freq.[a]	FT-IR	FT-Raman	
A''	ν_1	54	0.020	0.476	54	36			$\tau_{CCCC}(10)+\tau_{CCCH}(17)+\tau_{CCCN}(13)+\tau_{CCHN}(10)+\tau_{CCCF}(36)$
A''	ν_2	59	0.100	1.105	58	57			$\tau_{CCCC}(20)+\tau_{CCCH}(19)+\tau_{CCCN}(18)+\tau_{CCHN}(13)+\tau_{CCCF}(20)$
A''	ν_3	67	0.231	0.048	66	60			$\tau_{CCCH}(43)+\tau_{CCHN}(44)$
A''	ν_4	129	0.295	0.557	128	129			$\tau_{CCCC}(18)+\tau_{CCCH}(22)+\tau_{CCCN}(18)+\tau_{CCHN}(12)+\tau_{CCCF}(9)$
A'	ν_5	132	0.257	0.429	131	132			$\tau_{CCCC}(18)+\tau_{CCCH}(22)+\tau_{CCCN}(19)+\tau_{CCHN}(12)+\tau_{CCCF}(10)$
A''	ν_6	168	1.242	0.501	167	165		148 m	$\tau_{CCCC}(29)+\tau_{CCCH}(17)+\tau_{CCCN}(23)+\tau_{CCCF}(15)$
A''	ν_7	184	0.318	0.279	183	183		199 m	$\tau_{CCCC}(31)+\tau_{CCCH}(12)+\tau_{CCCN}(30)+\tau_{CCHN}(10)$

A"	ν_8	260	0.142	0.781	259	262		245 m	$\delta_{CCC}(19)+\delta_{CCN}(11)+\delta_{CCF}(10)+\tau_{CCNH}(17)$
A'	ν_9	276	0.259	0.392	274	276			$\tau_{CCCC}(24)+\tau_{CCCH}(22)+\tau_{CCCN}(23)$
A"	ν_{10}	285	0.847	1.144	284	289		283 m	$\tau_{CCCC}(10)+\tau_{CCCH}(11)+\tau_{CCCN}(14)+\tau_{CCNH}(25)$
A'	ν_{11}	309	1.552	0.394	307	314		310 s	$\tau_{CCCC}(10)+\tau_{CCCH}(10)+\tau_{CCNH}(39)$
A'	ν_{12}	330	4.215	0.308	328	331		334 m	$\tau_{CCCC}(12)+\tau_{CCNH}(41)$
A"	ν_{13}	357	0.314	0.792	355	358			$\delta_{CCC}(13)+\tau_{CCCC}(19)+\tau_{CCCH}(13)+\tau_{CCCN}(13)$
A'	ν_{14}	370	7.429	0.440	368	374		372 m	$\tau_{CCCC}(19)+\tau_{CCCH}(14)+\tau_{CCCN}(14)+\tau_{CCNH}(33)$
A"	ν_{15}	453	0.413	3.426	451	454			ν_{CC} $(13)+\delta_{CCC}(17)+\delta_{CCH}(10)+\delta_{CCN}(17)$
A'	ν_{16}	478	7.758	0.941	475	473		465 s	$\tau_{CCCC}(24)+\tau_{CCCH}(18)+\tau_{CCCN}(16)+\tau_{CCNH}(12)+\tau_{CCCF}(12)$
A"	ν_{17}	495	0.372	1.551	492	492			$\delta_{CCC}(14)+\delta_{CCH}(10)+\delta_{CCN}(13)+\delta_{CCF}(10)+\tau_{CCCF}(16)$
A'	ν_{18}	524	37.43	1.614	521	496		500 m	$\tau_{CCCC}(17)+\tau_{CCCH}(11)+\tau_{CCCN}(10)+\tau_{CCNH}(27)$
A'	ν_{19}	528	1.548	0.783	525	527		511 m	$\tau_{CCCC}(22)+\tau_{CCCH}(21)+\tau_{CCCN}(21)$
A"	ν_{20}	535	11.29	1.303	532	534		546 m	$\delta_{CCC}(11)+\tau_{CCCC}(10)+\tau_{CCCH}(12)+\tau_{CCCN}(11)+\tau_{CCNH}(17)$
A'	ν_{21}	546	16.48	3.182	543	545	563 m	561 m	$\delta_{CCC}(11)+\tau_{CCCC}(14)+\tau_{CCNH}(22)$
A"	ν_{22}	584	7.882	0.513	581	581	580 vw		$\tau_{CCCC}(24)+\tau_{CCCH}(17)+\tau_{CCCN}(11)+\tau_{CCNH}(17)$
A'	ν_{23}	590	5.028	1.585	587	590			$\delta_{CCC}(15)+\tau_{CCCC}(15)+\tau_{CCCH}(10)$
A"	ν_{24}	625	5.617	0.533	622	625	605 s	607 m	$\tau_{CCCC}(15)+\tau_{CCCH}(20)+\tau_{CCCN}(30)+\tau_{CCNH}(12)$
A'	ν_{25}	667	4.708	1.625	663	669			$\delta_{CCC}(15)+\delta_{CCH}(10)+\delta_{CCN}(10)+\tau_{CCCN}(10)$
A"	ν_{26}	692	0.685	0.198	689	692	679 vs	684 m	$\tau_{CCCC}(24)+\tau_{CCCH}(18)+\tau_{CCCN}(16)+\tau_{CCNH}(12)+\tau_{CCCF}(12)$
A'	ν_{27}	715	0.704	2.694	711	716	732 w	735 m	ν_{CC} $(15)+\delta_{CCC}(16)+\delta_{CCH}(10)+\delta_{CCN}(10)$
A"	ν_{28}	755	8.877	0.719	751	754	771 vs	762 m	$\tau_{CCCC}(13)+\tau_{CCCH}(45)+\tau_{CCCN}(20)$
A'	ν_{29}	818	3.869	0.901	814	820			$\tau_{CCCC}(22)+\tau_{CCCH}(24)+\tau_{CCCN}(13)+\tau_{CCNH}(10)$
A"	ν_{30}	821	4.431	1.664	816	825	825 vs		$\tau_{CCCC}(16)+\tau_{CCCH}(22)+\tau_{CCCN}(12)+\tau_{CCNH}(11)$
A'	ν_{31}	829	3.605	0.861	825	839	842 s	836 vw	$\tau_{CCCC}(21)+\tau_{CCCH}(25)+\tau_{CCCN}(16)+\tau_{CCNH}(24)$
A"	ν_{32}	861	3.162	0.574	856	862	872 m		ν_{CC} $(14)+\delta_{CCC}(22)+\delta_{CCH}(20)+\delta_{CCN}(10)$
A'	ν_{33}	915	0.850	0.344	910	914	930 w		$\tau_{CCCC}(14)+\tau_{CCCH}(52)+\tau_{CCHN}(16)$
A"	ν_{34}	962	0.642	0.310	957	959			$\tau_{CCCC}(15)+\tau_{CCCH}(56)+\tau_{CCHH}(15)$
A'	ν_{35}	967	3.711	0.394	962	971			$\nu_{CC}(9)+\delta_{CCC}(12)+\delta_{CCH}(22)+\delta_{CCN}(10)+\tau_{CCCH}(13)+\tau_{CCHN}(10)$
A'	ν_{36}	981	7.069	0.103	976	984	993 s	993 m	$\nu_{CC}(13)+\delta_{CCC}(13)+\delta_{CCH}(20)+\delta_{CCN}(10)+\tau_{CCCH}(10)$
A"	ν_{37}	1012	0.751	0.012	1007	1026			$\delta_{CCH}(20)+\tau_{CCCH}(27)+\tau_{CCCN}(18)+\tau_{CCHN}(10)$
A'	ν_{38}	1057	6.566	2.253	1052	1051			$\nu_{CC}(13)+\delta_{CCC}(12)+\delta_{CCH}(25)+\delta_{CN}(11)$
A"	ν_{39}	1065	12.98	1.076	1060	1062			$\nu_{CC}(18)+\delta_{CCC}(11)+\delta_{CCH}(24)$
A'	ν_{40}	1097	18.23	1.021	1091	1085	1076 vs	1077 m	$\nu_{CC}(15)+\delta_{CCC}(11)+\delta_{CCH}(18)+\delta_{CN}(14)$

A'	ν_{41}	1130	30.2	0.562	1124	1106			$\nu_{CC}(13)+\delta_{CCC}(11)+\delta_{CCH}(19)+\tau_{CCCF}(14)$
A'	ν_{42}	1149	76.91	0.675	1143	1112	1117 vs		ν_{CF} $(22)+\delta_{CCF}(10)+\tau_{CCCC}(12)+\tau_{CCCF}(24)$
A'	ν_{43}	1155	3.657	1.666	1149	1161	1143 s	1144 m	$\nu_{CC}(11)+\delta_{CCC}(10)+\delta_{CCH}(45)$
A'	ν_{44}	1163	11.66	0.434	1157	1170	1189 m	1182 m	$\nu_{CC}(13)+\delta_{CCC}(10)+\delta_{CCH}(37)$
A'	ν_{45}	1202	4.782	0.757	1196	1209	1228 m.sh	1228 m	$\nu_{CC}(15)+\delta_{CCC}(20)+\delta_{CCH}(28)+\delta_{CCN}(9)$
A'	ν_{46}	1256	0.527	0.857	1249	1252		1259 m	$\nu_{CC}(23)+\delta_{CCC}(12)+\delta_{CCH}(26)$
A"	ν_{47}	1281	100	8.203	1274	1266	1308 vs		$\nu_{CC}(19)+\nu_{CF}(19)+\delta_{CCC}(14)+\delta_{CCH}(26)$
A'	ν_{48}	1328	8.533	3.011	1321	1320		1309 s	$\nu_{CC}(21)+\delta_{CCC}(10)+\delta_{CCH}(23)$
A'	ν_{49}	1338	0.613	7.879	1331	1333	1332 vw		$\nu_{CC}(17)+\delta_{CCH}(32)+\delta_{HCH}(24)$
A'	ν_{50}	1360	6.484	54.59	1353	1357	1353 m.sh	1352 vs	$\nu_{CC}(35)+\delta_{CCC}(14)+\delta_{CCH}(20)$
A'	ν_{51}	1383	6.340	2.339	1376	1377		1375w	$\nu_{CC}(14)+\delta_{CCH}(14)+\delta_{CN}(16)+\delta_{HCH}(19)+\tau_{CCCH}(10)+\tau_{CCHN}(10)$
A'	ν_{52}	1401	6.917	22.29	1394	1423	1421 vw	1421 m	$\nu_{CC}(11)+\delta_{CCH}(14)+\delta_{HCH}(23)+\tau_{CCCH}(13)+\tau_{CCHN}(13)$
A'	ν_{53}	1411	1.967	5.709	1404	1428		1434 m	$\delta_{CCH}(9)+\delta_{HCH}(34)+\tau_{CCCH}(24)+\tau_{CCHN}(24)$
A'	ν_{54}	1421	2.239	17.66	1414	1441	1442 m	1441 m	$\nu_{CC}(22)+\delta_{CCC}(19)+\delta_{CCH}(27)$
A"	ν_{55}	1462	2.961	1.354	1454	1462			$\nu_{CC}(22)+\delta_{CCC}(13)+\delta_{CCH}(32)$
A'	ν_{56}	1510	17.10	0.910	1502	1501	1517 s	1525 m	$\nu_{CC}(26)+\delta_{CCC}(12)+\delta_{CCH}(30)$
A'	ν_{57}	1571	24.87	13.62	1563	1557	1569 vs	1572 s	$\nu_{CC}(34)+\delta_{CCC}(18)+\delta_{CCH}(19)+\delta_{CCN}(11)$
A'	ν_{58}	1584	14.86	2.581	1576	1585	1592 vs	1594 m	$\nu_{CC}(16)+\delta_{CCC}(10)+\delta_{CCH}(13)+\delta_{CNH}(12)+\delta_{HNH}(14)+\tau_{CCNH}(15)$
A'	ν_{59}	1609	36.23	4.025	1601	1603	1619 s	1621 m	$\nu_{CC}(21)+\delta_{CCC}(13)+\delta_{CCH}(22)+\tau_{CCNH}(11)$
A'	ν_{60}	1619	46.79	12.29	1611	1615	1638 s	1637 m	$\nu_{CC}(27)+\delta_{CCC}(17)+\delta_{CCH}(16)$
A'	ν_{61}	2939	5.973	100	2924	2933	2924 m	2925 m	$\nu_{CH}(88)$
A'	ν_{62}	2996	4.207	43.04	2980	2979	2956 vw	2964 m	$\nu_{CH}(76)$
A'	ν_{63}	3057	1.382	22.50	3041	3039			$\nu_{CH}(77)$
A"	ν_{64}	3072	4.883	46.55	3056	3062			$\nu_{CH}(71)$
A'	ν_{65}	3084	1.362	17.98	3068	3072		3072 m	$\nu_{CH}(78)+\delta_{CCC}(10)$
A'	ν_{66}	3104	4.864	58.35	3088	3091		3099 vw	$\nu_{CH}(81)$
A'	ν_{67}	3128	0.717	61.78	3112	3114	3252 m		$\nu_{CH}(79)$
A'	ν_{68}	3443	6.661	71.51	3426	3472	3383 s	3388 m	$\nu_{NH}(87)$
A'	ν_{69}	3541	4.892	21.71	3524	3569	3494 s		$\nu_{NH}(84)$

vs: very strong. ms: medium strong. s: strong. w: weak. vw: very weak.ν: stretching. t: torsion. γ: out of plane stretching. δ: in plane bending
[a] Obtained from the wavenumbers calculated at 0.970 for cc-pVDZ. 0.965 for cc-pVTZ. and 0.969 for cc-pVQZ basis sets [36].
[b] Relative absorbtion intensities and Relative Raman activities normalized with highest peak absorption equal to 100.
[c] Total energy distribution calculated B3LYP cc-pVDZ level of theory. Only contributions≥ 10 % are listed.

Celal Bayar University Journal of Science
Volume 13, Issue 4, p 851-861

5. HOMO-LUMO analysis

HOMO (Highest Occupied Molecular Orbital) and LUMO (Lowest Unocupied Molecular Orbital) are known as Molecular orbitals. They were very important electronic parameters for chemist and physicist. The LUMO are known as the inner-most orbital containing free places to accept electrons. It defines the ability of accepting electron. HOMO can be considered the outermost orbital containing electrons. It characterizes the ability of giving electron. HOMO and LUMO energies of chemical compounds are important quantum mechanical parameters. They are very useful to explain its reactivity. The plots of HOMO, HOMO-1, and LUMO, LUMO+1, molecular orbitals for the AMTQ were given in Figure 4.

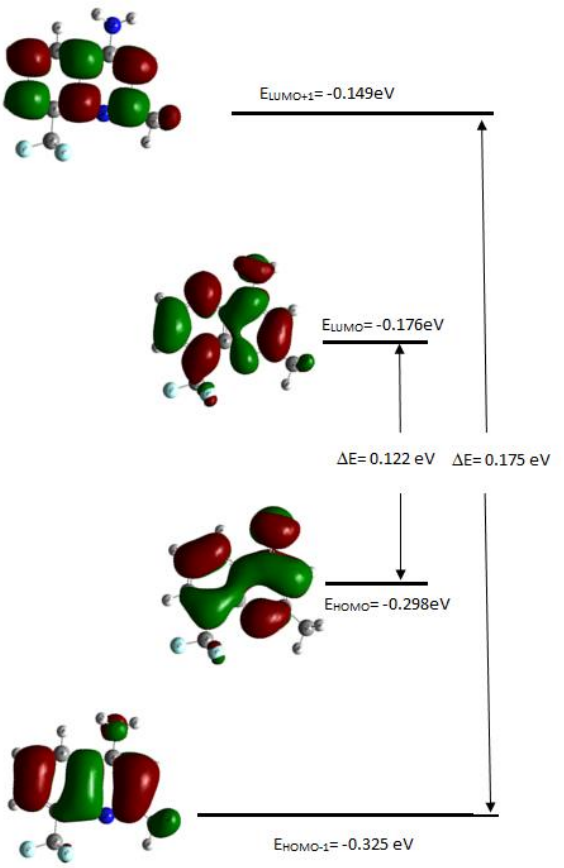

Figure 4. HOMO and LUMO plot of of 4-amino-2-methyl-8-(trifluoromethyl)quinolone molecule (B3LYP / cc-pVDZ)

6. Nuclear Magnetic Resonance Spectra

Significant progress has been achieved in chemical shifts calculations which aids in spectral assignment and structural elucidation. Meanwhile, the Gauge Invariant Atomic Orbitals (GIAO) approach [37,38] that uses density functional theory, DFT-B3LYP and DFT-B3PW91 calculations have afforded excellent agreement with experimental NMR spectral analysis [39-41]. Therefore, we have used the optimized geometry of AMTQ structure from B3LYP using cc-pVDZ, cc-pVTZ and cc-pVQZ basis sets in DMSO solution for further optimization, while employing Tomasi's Polarized Continuum Model (PCM) [19]. The ^{13}C NMR nuclear shielding constants were predicted using GIAO approximation with the above method. The calculated ^{1}H and ^{13}C absolute isotropic shielding (si, ppm) parameters were converted into ^{1}H and ^{13}C chemical shifts (δ_{calc}, ppm.) using ($\delta_{calc}=\delta_{TMS}-\delta_{i}$). The experimental peaks along with the simulated ^{1}H (a) and ^{13}C (b) nuclear magnetic resonance (NMR) spectra of 4-amino-2-methyl-8-(trifluoromethyl)quinoline molecule shown in Figure 5.

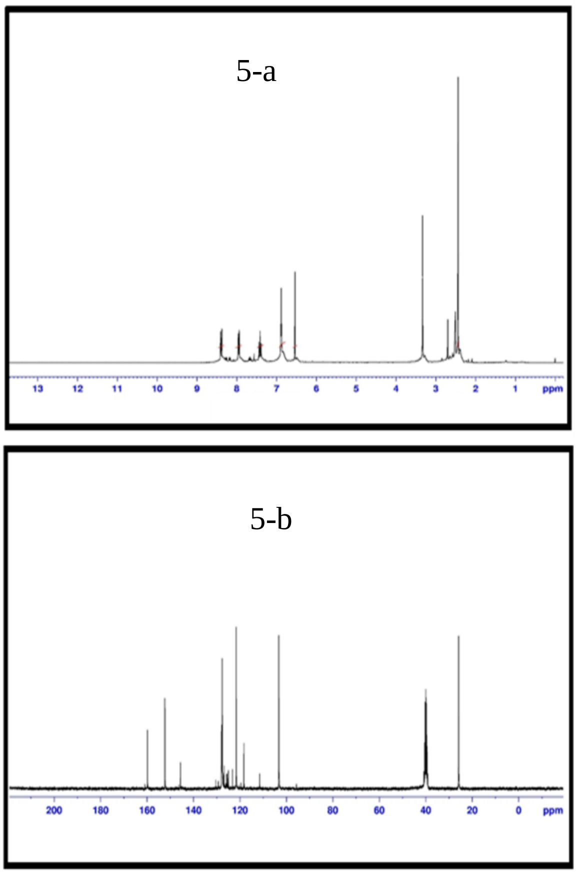

Figure 5. ^{1}H (a) and ^{13}C (b) NMR spectra of 4-amino-2-methyl-8-(trifluoromethyl)quinoline

^{1}H and ^{13}C experimental and theoretical NMR chemical shifts are listed in Table 3 with AMTQ sample dissolved in DMSO-d6. According to the ^{13}C NMR spectrum, the signal observed at 160.9 ppm are undoubtedly assigned to the C_5 (C_5-C_{17}-H_3) which agrees with B3LYP/cc-pVDZ, cc-pVTZ and cc-pVQZ predicted values at 161.9 ppm, 169.1 ppm and 172.4 ppm, respectively. Similarly, the signals observed at 159.8 ppm have been assigned to C_2 and C_2 (coordinated to the amino group) in agreement with estimated values at 160.6 ppm using B3LYP/ cc-pVQZ. ^{1}H NMR spectra interpreted significantly in an attempt to measure the possible different effects appearing on the chemical shift values of protons. Observed proton chemical shift values are in the region

8.406-2.441 ppm. In the proton NMR spectra, the signals are observed at 6.883 (H_7), 7.940 (H_{12}), 8.379 (H_6) and 8.406 (H_{25}) ppm. Hydrogen atoms attached to quinoline ring. The methyl hydrogen atoms are H_{18}, H_{19} and H_{20} and exhibit shift at 2.515, 2.509 and 2.441 ppm, respectively. The chemical shifts of the H_{15} and H_{16}, which is attached to N_{14}, appeared at 3.400 ppm and 3.332 ppm by experimental data. We note that the experimental ^1H NMR data agrees with them of the theoretical predicted.

Table 3. Theoretical and experimental ^1H and ^{13}C spectra of the title molecule (with respect to TMS, all values in ppm)

	Theoretical (B3LYP)			Exp.		Theoretical (B3LYP)			Exp.
	cc-pVDZ	cc-pVTZ	cc-pVQZ			cc-pVDZ	cc-pVTZ	cc-pVQZ	
H_{25}	8.028	8.410	8.492	8.406	C_5	161.9	169.1	172.4	160.9
H_6	7.849	8.206	8.263	8.379	C_2	149.4	158.2	160.6	159.8
H_{12}	7.430	7.723	7.770	7.940	C_4	148.3	155.4	157.9	152.2
H_7	6.474	6.831	6.883	6.883	C_9	134.4	139.1	142.0	145.6
H_{15}	3.954	4.429	4.563	3.400	C_{21}	131.4	139.3	140.1	128.0
H_{16}	3.385	3.896	4.064	3.332	C_{10}	129.1	135.6	137.7	127.9
H_{18}	2.825	2.940	2.949	2.515	C_8	124.5	130.3	132.5	127.8
H_{19}	2.817	2.946	2.957	2.509	C_{11}	123.4	128.8	130.8	127.6
H_{20}	2.651	2.925	2.980	2.441	C_3	121.5	125.7	128.1	121.6
					C_1	105.4	109.3	111.0	103.2
					C_{17}	29.05	29.81	29.55	25.82

7. Molecular Electrostatic Potential Maps

The molecular electrostatic potential (MEP) maps of ground state of AMTQ are shown in Fig. 6. In the organic molecules, the MEP is generally used as a reactivity map displaying. These regions are the most probable regions for the electrophilic attack. The MEP contour map provides a simple way to predict how different geometries could interact. The calculated 3D MEP contour map (red is negative, blue is positive) shows the negative regions. In the AMTQ molecule is mainly over the Nitrogen atoms. The electrostatic potential maps have been used for predicting sites.

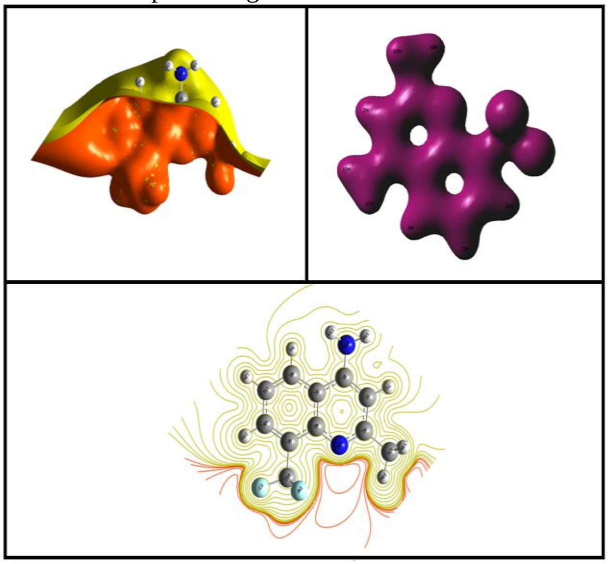

Figure 6. Molecular ESP mapped on the isodensity surface for 4-amino-2-methyl-8-(trifluoromethyl)quinolone molecule

8. Conclusion

This work deal with the vibrational, Nuclear Magnetic Resonance spectra, molecular structure and some electronic properties of AMTQ molecule by theoretical methods and experimental setup. The results of theoretical and experimental studies are combining with together. The most stable conformer of the AMTQ is predicted by DFT calculation. The ground state conformers of AMTQ are further studied using the Density Functional Theory at B3LYP with cc-pVQZ, cc-pVTZ and cc-pVDZ basis sets. The spectroscopic, structural and electronic properties of the ground state have been calculated by Gaussian09. The experimental work has focused on the assignment of the vibrational spectra from 400 to 4000 cm^{-1}. Computed results of the AMTQ are found to be in better agreement with the experimental findings.

References

1. Quinoline, Wikipedia, https://en.wikipedia.org/wiki/Quinoline, 2017, (accessed 20.05.2017).

2. Wang, L.Y., Chen, Q.W., Zhai, G.H., Wen, Z.Y., Zhang, Z.X., Theoretical study on the structures and absorption properties of styryl dyes with quinoline nucleus, *Dyes and Pigmentes*, 2007, 72, 357–362.

3. Dahule, H.K., Thejokalyani, N., Dhoble, S.J., Novel Br-DPQ blue light-emitting phosphors for OLED, *Luminescence*, 2014, 4, 405–410.

4. Ciobotaru, I.C., Polosan, S., Ciobotaru, C.C., Dual emitter IrQ(ppy)2 for OLED applications: Synthesis and spectroscopic analysis, *Journal of Luminescence*, 2014, 145, 259–262.

5. Camargo, H, Paolini, T.B., Niyama, E, Brito, H.F., Cremona, M, New rare-earth quinolinate complexes for organic light-emitting devices, *Thin Solid Films*, 2013, 528, 36–41.

6. Dereli, O, Erdogdu, Y, Gulluoglu, M.T., Ozmen, A, Sundaraganesan, N, Vibrational spectral and quantum chemical investigations of tert-butyl-hydroquinone, *Journal of Molecular Structure*, 2012, 1012, 168-176.

7. Dereli, O, Sudha, S, Sundaraganesan, N, Molecular structure and vibrational spectra of 4-phenylsemicarbazide by density functional method, *Journal of Molecular Structure*, 2011, 994, 379-386.

8. Yurdakul, Ş, Badoglu, S, An FT-IR and DFT study of the free and solvated 4-(imidazol-1-yl)phenol, *Spectrochimica Acta Part A: Molecular and Biomolecular Spectroscopy*, 2015, 150, 614-622.

9. Yurdakul, Ş, Badoglu, S, Ozkurt, L, An experimental and theoretical investigation of free Oxazole in conjunction with the DFT analysis of Oxazole $(H_2O)_n$complexes, *Spectrochimica Acta Part A: Molecular and Biomolecular Spectroscopy*, 2016, 162, 48-60.

10. Erdogdu, Y, Investigations of FT-IR, FT-Raman, FT-NMR spectra and quantum chemical computations of Esculetin molecule, *Spectrochimica Acta Part A: Molecular and Biomolecular Spectroscopy*, 2013, 106, 25-33.

11. Erdogdu, Y, Unsalan, O, Gulluoglu, M.T., FT-Raman, FT-IR spectral and DFT studies on 6, 8-dichloroflavone and 6, 8-dibromoflavone, *Journal of Raman Spectroscopy*, 2010, 41, 820-828.

12. Subashchandrabose, S, Saleem, H, Erdogdu, Y, Dereli, Ö, Thanikachalam, V, Jayabharathi, J, Structural, vibrational and hyperpolarizability calculation of (*E*)-2-(2-hydroxybenzylideneamino)-3-methylbutanoic acid, *Spectrochimica Acta Part A: Molecular and Biomolecular Spectroscopy*, 2012, 86, 231-241.

13. Sajan, D, Erdogdu, Y, Kuruvilla, T, Hubert Joe, I, Vibrational spectra and first-order molecular hyperpolarizabilities of p-hydroxybenzaldehyde dimer, *Journal of Molecular Structure*, 2010, 983,12-21.

14. Erdogdu, Y, Unsalan, O, Sajan, D, Gulluoglu, M.T., Structural conformations and vibrational spectral study of chloroflavone with density functional theoretical simulations, *Spectrochimica Acta Part A: Molecular and Biomolecular Spectroscopy*, 2010, 76, 130-136.

15. Erdoğdu, Y, Güllüoğlu, M.T., Yurdakul, Ş, Molecular structure and vibrational spectra of 1,3-bis(4-piperidyl)propane by quantum chemical calculations, *Journal of Molecular Structure*, 2008, 889, 361-370.

16. Frosch, T, Schmitt, M, Popp, J, Raman spectroscopic investigation of the antimalarial agent mefloquine, *Analytical and Bioanalytical Chemistry*, 2007, 387, 1749–1757.

17. Frosch, T, Popp, J, Structural analysis of the antimalarial drug halofantrine by means of Raman spectroscopy and density functional theory calculations, *Journal of Biomedical Optics*, 2010, 15 (4), 041516. doi:10.1117/1.3432656

18. Frosch, T, Schmitt, M, Schenzel, K, Faber, J.H., Bringmann, G, Kiefer, W, Popp, J, *In vivo* localization and identification of the antiplasmodial alkaloid dioncophylline A in the tropical liana *Triphyophyllum peltatum* by a combination of fluorescence, near infrared Fourier transform Raman microscopy, and density functional theory calculations, *Biopolymers*, 2006, 82, 295–300.

19. Frosch, T, Küstner, B, Schlücker, S, Szeghalmi, A, Schmitt, M, Kiefer, W, Popp, J, *Invitro* polarization-resolved resonance Raman studies of the interaction of hematin with the antimalarial drug chloroquine, *Journal of Raman Spectroscopy*, 2004, 35, 819–821.

20. Ulahannan, R.T., Panicker, C.Y., Varghese, H.T., Van Alsenoy, C, Musiol, R, Jampilek, J, Anto, P.L, Spectroscopic (FT-IR, FT-Raman) investigations and quantum chemical calculations of 4-hydroxy-2-oxo-1,2-dihydroquinoline-7-carboxylic acid, *Spectrochimica Acta Part A: Molecular and Biomolecular Spectroscopy*, 2014, 121, 404–414.

21. Frosch, T, Popp, J, Relationship between molecular structure and Raman spectra of quinolones, *Journal of Molecular Structure*, 2009, 924–926, 301–308.

22. Cînta-Pînzaru, S, Peica, N, Küstner, B, Schlücker, S, Schmitt, M, Frosch, T, Faber, J.H., Bringmann, G, Popp, J, FT-Raman and NIR-SERS characterization of the antimalarial drugs chloroquine and mefloquine and their interaction with hematin, *Journal of Raman Spectroscopy*, 2006, 37, 326–334.

23. Frosch, T, Schmitt, M, Bringmann, G, Kiefer, W, Popp, J, Structural Analysis of the Anti-Malaria Active Agent Chloroquine under Physiological Conditions, *Journal of Physical Chemistry B*, 2007, 111, 1815–1822.

24. Frosch, T, Schmitt, M, Popp, J, *In situ* UV Resonance Raman Micro-spectroscopic Localization of the Antimalarial Quinine in Cinchona Bark, *Journal of Physical Chemistry B*, 2007, 111, 4171–4177.

25. Fazal, E, Jasinski, J, Anderson, B, Kaur, M, Nagarajan, S, Sudha, B, Synthesis, Crystal and Molecular Structure Studies and DFT Calculations of Phenyl Quinoline-2-Carboxylate and 2-Methoxyphenyl Quinoline-2-Carboxylate; Two New Quinoline-2 Carboxylic Derivatives, *Crystals*, 2015, 5, 100- 115.

26. Diwaker, C.S., Chidan, Kumar, A, Chandraju, Kumar, S, Spectroscopic (FT-IR, ^{1}H, ^{13}C NMR and UV–vis) characterization and DFT studies of novel 8-((4-(methylthio)-2,5-diphenylfuran, *Spectrochimica Acta Part A: Molecular and Biomolecular Spectroscopy*, 2015, 150, 602–613.

27. Ulahannan, R.T., Panicker, C.Y., Varghese, H.T., Musiol, R., Jampilek, J., Alsenoy, C.V., War, J.A., Manojkumar T.K., Vibrational spectroscopic stu*dies* and molecular docking study of 2-[(*E*)-2-phenylethenyl]quinoline-5-carboxylic acid, *Spectrochimica Acta Part A: Molecular and Biomolecular Spectroscopy*, 2015, 150, 190–199.

28. Kulkarni, A, King, C, Butcher, R.J., Fortunak, M.D., 4,7-Dichloro-quinolone, *Acta Crystallographica*, 2012, E68, 1498.

29. Pereira, G.R., et al., 7-Chloroquinolinotriazoles: Synthesis by the azide–alkyne cycloaddition click chemistry, antimalarial activity, cytotoxicity and SAR studies, *European Journal of Medicinal Chemistry*, 2014, 73, 295–309.

30. Frisch, M.J., Trucks, G.W., Schlegel, H.B., Scuseria, G.E., Robb, M.A., Cheeseman, J.R., et al., Gaussian 09, revision A.2. Wallingford CT: Gaussian, Inc., 2009.

31. Pulay, P., Baker, J., Wolinski, K, Green Acres Road Suite A Fayettevile, Arkansas, 72703, USA, 2013.

32. Thanikachalam, V, Periyanayagasamy, V, Jayabharathi, J, Manikandan, G, Saleem, H, Subashchandrabose, S, Erdogdu, Y, FT-Raman, FT-IR spectral and DFT studies on (*E*)-1-4-nitrobenzylidenethiocarbonohydrazide, *Spectrochimica Acta Part A: Molecular and Biomolecular Spectroscopy*, 2012, 87, 86-95.

33. Roeges, N.P.G., A Guide to the Complete Interpretation of Infrared Spectra of Organic Structures, Wiley, New York, 1994.

34. Güllüoğlu, M.T., Erdogdu, Y, Yurdakul, Ş, Molecular structure and vibrational spectra of piperidine and 4-methylpiperidine by

density functional theory and ab initio Hartree–Fock calculations, *Journal of Molecular Structure*, 2007, 834, 540-547.

35. Erdogdu, Y, Güllüoğlu, M.T., Analysis of vibrational spectra of 2 and 3-methylpiperidine based on density functional theory calculations, *Spectrochimica Acta Part A: Molecular and Biomolecular Spectroscopy*, 2009, 74, 162-167.

36. CCCBDB listing of precalculated vibrational scaling factors NIST, http://srdata.nist.gov/cccbdb/vibscalejust.asp, 2017 (accessed 20.05.2017).

37. Ditchfield, J. R., Molecular Orbital Theory of Magnetic Shielding and Magnetic Susceptibility, *Journal of Chemical Physics*, 1972, 56, 5688

38. Wolinski, K, Hinton, J.F., Pulay, P, Efficient implementation of the gauge-independent atomic orbital method for NMR chemical shift calculations, *Journal of American Chemical Society*, 1990, 112 (23), 8251-8260.

39. Azizi, N, Rostami, A.A., Godarzian, A, ^{29}Si NMR Chemical Shift Calculation for Silicate Species by Gaussian Software, *Journal of Physical Society of Japan*, 2005, 74, 1609-1620.

40. Rohlfing, M, Leland, C, Allen, C, Ditchfield, R, Proton and carbon-13 chemical shifts: Comparison between theory and experiment, *Chemical Physics*, 1984, 87, 9-15.

41. Chesnut, D, Phung, C, Nuclear magnetic resonance chemical shifts using optimized geometries, *Journal of Chemical Physics* 1989; 91, 6238 – 6245